Conference paper

Maria Elisa Crestoni, Barbara Chiavarino and Simonetta Fornarini*

Nitrosyl–heme and anion–arene complexes: structure, reactivity and spectroscopy

Abstract: Two topics are selected and illustrated to exemplify (i) a biological and (ii) an organic ionic intermediate. The reactivity behavior of NO adducts with ferric and ferrous hemes has shown remarkable similarities when examined in the gas phase, demonstrating that the largely different NO affinity displayed in solution and in biological media is due to the different coordination environment. In fact, ferrous hemes present a vacant or highly labile axial coordination site, prone to readily bind NO. The vibrational signatures of the NO ligand have also been probed in vacuo for the first time in the nitrosyl complexes deriving from ferrous and ferric hemes under strictly comparable five-coordination at the metal center. Negatively charged σ-adducts, from the association of anions with 1,3,5-trinitrobenzene, an exemplary π-electron-deficient arene, have been probed by IRMPD spectroscopy and found to display variable binding motifs from a strongly covalent σ-adduct (Meisenheimer complex) to a weakly covalent σ-complex, depending on the anion basicity.

Keywords: gas phase; ICPOC-22; IRMPD spectroscopy; mass spectrometry; Meisenheimer complexes; nitrosylation reaction.

DOI 10.1515/pac-2014-1203

Introduction

The past few decades have witnessed a wealth of fundamental knowledge in physical organic chemistry gained through the study of ionic reaction mechanisms in the gas phase. The gaseous environment has offered an ideal medium whereby charged reaction intermediates can be investigated to unveil intrinsic reactivity or catalytic role. The pioneering development and implementation of a variety of techniques, mainly based on mass spectrometry, has allowed to unravel elementary reactions at a molecular level and to characterize key reaction intermediates, elucidating their structure and thermochemical properties [1–9]. Within the session theme, namely the gas phase chemistry of organic and biological ions, the focus of this contribution is centered on two species, namely the heme nitrosyl complexes and the adducts of negative ions with π-acidic aromatic systems selected to exemplify (i) a biological and (ii) an organic ionic intermediate, respectively. Heme nitrosyl complexes are central intermediates in bioinorganic chemistry because the bonding of nitric oxide (NO) to the heme prosthetic group is responsible for a large part of the biological functions of NO. This endogenously formed diatomic molecule is involved, inter alia, in blood pressure control, neurotransmission

Article note: A collection of invited papers based on presentations at the 22nd IUPAC International Conference on Physical Organic Chemistry (ICPOC-22), Ottawa, Canada, August 10–15, 2014.

***Corresponding author: Simonetta Fornarini,** Dipartimento di Chimica e Tecnologie del Farmaco, Università degli Studi di Roma La Sapienza, P.le A. Moro 5, I-00185, Roma, Italy, e-mail: simonetta.fornarini@uniroma1.it
Maria Elisa Crestoni and Barbara Chiavarino: Dipartimento di Chimica e Tecnologie del Farmaco, Università degli Studi di Roma La Sapienza, P.le A. Moro 5, I-00185, Roma, Italy

and immune response which explains the conspicuous effort directed at characterizing the structural and reactivity features of heme nitrosyl complexes as either model complexes in solution or in heme proteins [10–12]. Figure 1 shows the crystal structure of a nitrophorin–NO complex. The nitrophorins are released by the salivary glands of blood-sucking insects and use iron(III)-heme to deliver nitric oxide at the site of the bite, ensuring vasodilation and maintaining blood flow. The reactivity of NO within heme proteins is known to be affected by the presence and number of axial ligands and by the interaction with functional groups lining the heme pocket. However, a most important factor in determining the affinity towards NO appears to be due to the metal oxidation state. Iron(II) heme proteins and model complexes in solution react with NO remarkably faster than the respective iron(III) species with second order rate constants in the range of 10^3–10^9 M^{-1} s^{-1} [10]. A similarly high difference affects the association equilibrium constant, K. For example, NO binds to myoglobin [holding iron(II)-heme] with a K value 8 orders of magnitude higher than the one pertaining to metmyoglobin [holding iron(III)-heme]. This largely different behavior has been explained by the fact that the faster forward rate for iron(II)-heme models relative to the iron(III)-hemes is due to the five-coordinate nature of the former. In the case of iron(III)-hemes, which exist as diaquo complexes in water, the forward NO substitution mechanism is dominated by ligand dissociation. It was thus deemed important to ascertain the factors behind the apparently lower affinity of NO towards iron(III)-hemes. In the isolated gas phase one can deal with iron(II)/(III)-hemes in a strictly comparable coordination environment, unveiling the neat interaction of NO with a heme center [13]. An overview is presented of our gas phase studies which have comprised: (i) selecting proper precursors to form the ions of interest; (ii) surveying the plausible structures that may account for the sampled ions by computational approaches; (iii) examining the gas phase reactivity (iv) probing vibrational features to further characterize electronic and geometric structures [14–19].

The second class of charged complexes arises from the interaction of anions with π-receptor arenes. The so-formed species are important in many areas ranging from organic reactivity to supramolecular chemistry and to biochemistry. Figure 2 shows exemplary anionic σ-adducts, known as Jackson–Meisenheimer

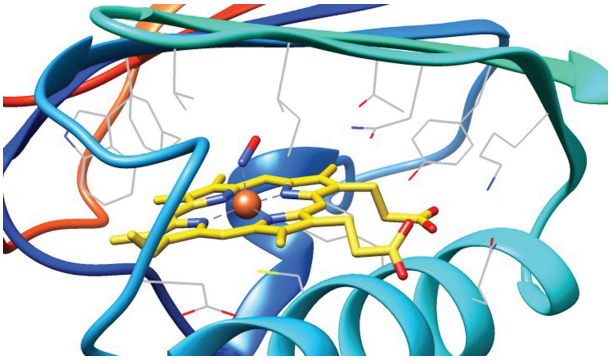

Fig. 1: An image of the active site region of the crystal structure of cimex nitrophorin complex with NO (PDB code: 1YJH).

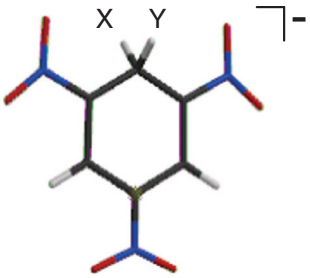

Fig. 2: Anionic σ-complex.

complexes, key intermediates in the S_NAr mechanism of nucleophilic aromatic substitution [20]. The first complex isolated by Meisenheimer in 1902 and characterized by the crystal structure responds to X = Y = OCH_3. A relatively novel, structurally diagnostic tool has recently allowed us to ascertain the bonding features of the gaseous adducts of simple anions (OH^-, OCH_3^-, $OC_2H_5^-$, F^-, Cl^-, Br^-, I^-, CN^-) with a π-acidic arene (1,3,5-trinitrobenzene, TNB) [21–24].

Ferrous and ferric hemes: genuine four-coordinate complexes in the gas phase

The naked heme ion holding iron(III) coordinated by the dianion of protoporphyrin IX, Fe^{III}-$heme^+$, is delivered in the gas phase directly by electrospray ionization (ESI) of a hemin chloride solution (Fe^{III}-$heme^+Cl^-$). Obtaining a heme type cation holding iron(II) is less straightforward to achieve in the gas phase. We have taken advantage of an approach based on the collision induced dissociation of the charged species from electrospray ionization of microperoxidase (MP-11, the heme undecapeptide derived from enzymatic cleavage of cytochrome c). The so-formed species, corresponding formally to neutral Fe^{II}-heme with an excess unit positive charge resulting from the addition of a proton, Fe^{II}-$hemeH^+$, has been characterized both computationally by density functional theory (DFT) and experimentally using FT-ICR mass spectrometry [14]. The observed ion chemistry towards hydrogen-deuterium exchange supports very similar features for both Fe^{III}-$heme^+$ and Fe^{II}-$hemeH^+$ ions. In fact, H/D exchange occurs only with relatively basic reagents, acetic acid and ammonia, and is limited to just two events. Also the rate constants for the consecutive steps of Scheme 1 are comparable, differing by less than a factor of 2.

The results are consistent with the two propionic acid functionalities on the periphery of the porphyrin being involved in the exchange process. These groups are clearly not involved in the protonation of neutral Fe^{II}-heme to form Fe^{II}-$hemeH^+$ ions. In contrast, the reactivity towards ligand addition is markedly different for Fe^{III}-$heme^+$ and Fe^{II}-$hemeH^+$ ions. For example, the addition of acetic acid and ammonia to Fe^{III}-$heme^+$ in the gas phase is characterized by a reaction efficiency of 0.6 and 2.0, respectively, while Fe^{II}-$hemeH^+$ ions are unreactive [14]. These findings confirm the higher quest for axial coordination by hard ligands displayed by ferric heme when the two species, Fe^{III}-$heme^+$ and Fe^{II}-$hemeH^+$ ions, are examined in the same coordination environment, namely as genuine four-coordinate complexes. In order to further ascertain the structural features of Fe^{II}-$hemeH^+$ ions, DFT calculations were performed to evaluate several conceivable isomers differing for the position of the additional proton. The most stable among the species investigated is the one corresponding to protonation at the β carbon atom of a vinyl group (Fig. 3) while complete structural relaxation in three different spin states resulted in the triplet state to be lowest in energy. The spin density distribution

$$Fe^{III}\text{-}heme^+(d_0) \underset{}{\overset{k_1}{\rightleftharpoons}} Fe^{III}\text{-}heme^+(d_1) \overset{k_2}{\rightleftharpoons} Fe^{III}\text{-}heme^+(d_2) \quad (1a)$$

$$Fe^{II}\text{-}hemeH^+(d_0) \underset{}{\overset{k_1}{\rightleftharpoons}} Fe^{II}\text{-}hemeH^+(d_1) \overset{k_2}{\rightleftharpoons} Fe^{II}\text{-}hemeH^+(d_2) \quad (1b)$$

Scheme 1: H/D exchange reactions of Fe^{III}-$heme^+$ and Fe^{II}-$hemeH^+$ ions.

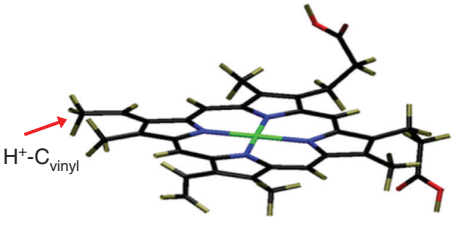

Fig. 3: Structure of the most stable isomer of Fe^{II}-$hemeH^+$.

shows an excess of α spin at the central iron atom and an excess of β spin on the porphyrin ligand, in particular on the former vinyl group in protoporphyrin IX which acquires ethyl radical character. Gaseous Fe^{II}-$hemeH^+$ ions may then be described as species possessing iron(III) character to a certain extent, due to partial electron transfer from the metal to the protonated porphyrin unit, as illustrated in a $[Fe^{III}\text{-}hemeH^{\bullet}]^+$ formal description. The ion chemistry of $[Fe^{II}\text{-}hemeH]^+$ ions, however, has shown notable differences with respect to the one displayed by $[Fe^{III}\text{-}heme]^+$ in the ligand addition reactions [14].

Kinetics and thermodynamics of nitric oxide binding to ferrous and ferric hemes: comparable behavior in the isolated ions

A variety of ligands have been sampled for their binding properties to gaseous Fe^{III}-$heme^+$ and Fe^{II}-$hemeH^+$ ions. The ligands have been selected among substrate molecules of heme proteins or among model compounds endowed with functional groups that are present in the heme protein environment (e.g., amino or aza groups). A correlation is found between the Gibbs free energy for ligand binding to the heme and the gas phase basicity towards the proton (GB). However, a notable exception is presented by nitric oxide. This diatomic biomolecule displays equilibrium constants for the association to Fe^{III}-$heme^+$ and Fe^{II}-$hemeH^+$ ions that are remarkably high, much higher than expected on the basis of the scant GB of NO. It is clear that NO displays exceptional binding properties towards ferrous and ferric hemes. Even more noteworthy is the finding that the two ions share very similar values both in the association equilibrium constant and in the binding kinetics. The equilibrium constants have been obtained by two independent procedures [15, 16]. In the first one, ligand exchange equilibria have been set up in the FT-ICR cell and a ladder of ligand exchange free energies has been collected providing absolute values for the free energies of NO addition, anchored to the neat addition equilibria of weakly bound ligands. In the second one, the equilibrium constants were obtained by the ratio of the rate constants for the forward and reverse reaction (Scheme 2). The good agreement between thermodynamic data obtained by the two methods confirms that the ionic species are in thermal equilibrium with the environment.

As shown by the data summarized in Table 1, iron(II)- and iron(III)-hemes behave very similarly in their gas phase reaction with NO. It may be underlined once again that the sampled complexes are both four coordinate at the metal center so that their reactivity properties are to be related to the different oxidation state and electronic structure. In this case, nitric oxide performs as an equally powerful ligand towards both Fe^{III}-$heme^+$ and Fe^{II}-$hemeH^+$ ions, irrespective of the different spin change along the reaction coordinate for the bond formation process. The remarkable similarities observed in the nitrosylation reaction have then spurred further efforts to characterize the nature of the ferrous and ferric heme nitrosyl complexes formed in the gas phase reaction. DFT calculations and vibrational spectroscopy of the gaseous ions have provided thoroughly consistent information.

$$Fe^{II}\text{-}hemeH^+ \{\text{or } Fe^{III}\text{-}heme^+\} + NO \underset{k_{off}}{\overset{k_{on}}{\rightleftharpoons}} Fe^{II}\text{-}hemeH(NO)^+ \{\text{or } Fe^{III}\text{-}heme(NO)^+\}$$

Scheme 2: Reaction of NO with Fe^{III}-$heme^+$ and Fe^{II}-$hemeH^+$ ions.

Table 1: Kinetics and equilibrium data for NO binding to gaseous iron (II/III) heme ions at 300 K [16].

Reactant ion	$k_{on}/10^{-11}$ cm^3 molecule^{-1} s^{-1}	$k_{off}/10^{-3}$ s^{-1}	$K/10^{11}$ atm^{-1}
Fe^{III}-$heme^+$	2.2	0.9	5.3
Fe^{II}-$hemeH^+$	3.3	0.8	5.7

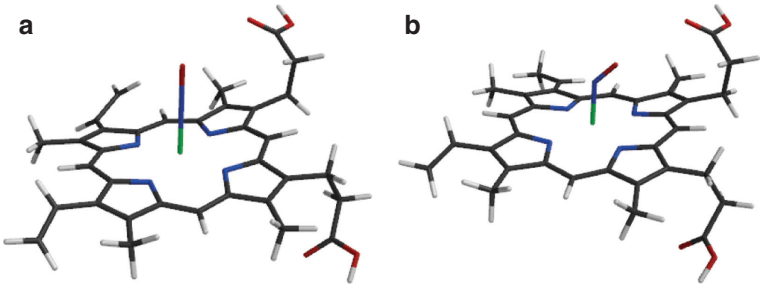

Fig. 4: Structure of Fe^{III}-heme(NO)$^+$ (a) and Fe^{II}-hemeH(NO)$^+$ (b) ions.

Computational survey of ferrous and ferric heme nitrosyl complexes

The formation of NO adducts to Fe^{III}-heme$^+$ and Fe^{II}-hemeH$^+$ ions has been examined also by DFT calculations, to provide an independent source of insight about the features of the investigated complexes. Care has to be exercised, though, because these systems are unusually challenging for DFT methods [25, 26]. The ground state of both Fe^{III}-heme$^+$ and Fe^{II}-hemeH$^+$ ions is recognized to be an intermediate spin state, namely quartet and triplet, respectively. NO is a strong field ligand yielding low spin adducts with Fe^{III}-heme$^+$ and Fe^{II}-hemeH$^+$, in singlet and doublet ground state, respectively [16]. The NO diatomic is axially bound in an end-on configuration (η^1-NO). The most notable feature in the optimized geometries (Fig. 4) is the Fe–N–O angle which is equal to 178.6° in the NO complex with ferric heme and 145.6° in the complex with ferrous heme. Binding energies were obtained by comparing the energy of the nitrosyl complex with those of the optimized fragments, all species in their lowest energy spin state. By these means the NO binding energies to Fe^{III}-heme$^+$ and Fe^{II}-hemeH$^+$ ions turn out to be 144 and 140 kJ mol^{-1}, respectively [16]. These remarkably close values are fully consistent with the approximately equal free energies for NO addition determined experimentally by FT-ICR mass spectrometry. However, the nitrosyl complexes are clearly different in terms of geometry and electronic structure and further characterization has been sought experimentally relying on vibrational spectroscopy.

Electronic structure and ligand vibrations in FeNo porphyrin complexes

Vibrational spectroscopy of gaseous ions is not amenable to a conventional absorption experiment because the ion density is too low. IR photon absorption is rather monitored in an indirect way through the photofragmentation process activated when the radiation is resonant with active vibrational modes of the sampled ion. The ensuing 'action' spectroscopy relies on an IR (multiple) photon dissociation (IRPD or IRMPD) process whose yield is monitored as a function of the IR wavenumber [27, 28]. The heme nitrosyl complexes undergo loss of NO as the only photofragmentation path (Scheme 3).

The reported NO binding energies require the nitrosyl complex to absorb more than ten photons in the 1000–2000 cm^{-1} wavenumber range in order to reach the threshold energy for dissociation. The IRMPD spectrum of Fe^{III}-heme(NO)$^+$ recorded at the CLIO free electron laser (FEL) facility is shown in Fig. 5a [17]. The

$$Fe^{II}\text{-hemeH(NO)}^+ \{\text{or } Fe^{III}\text{-heme(NO)}^+\} \xrightarrow{nh\nu} Fe^{II}\text{-hemeH}^+ \{\text{or } Fe^{III}\text{-heme}^+\} + NO$$

Scheme 3: IR multiple photon fragmentation process of the nitrosyl complexes from Fe^{III}-heme$^+$ and Fe^{II}-hemeH$^+$ ions.

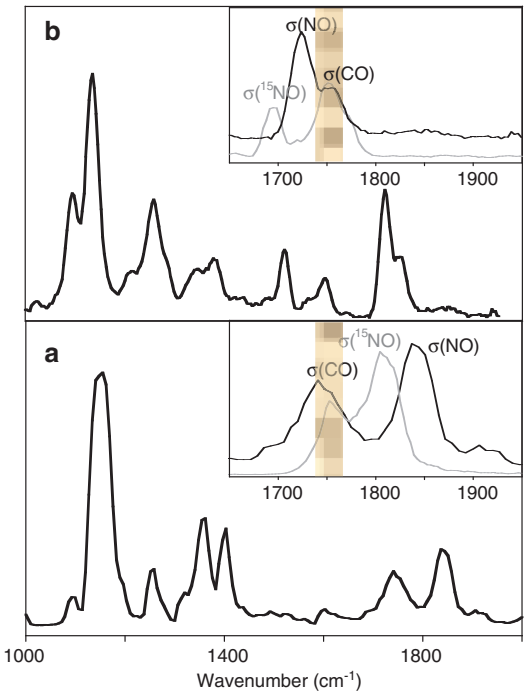

Fig. 5: IRMPD spectra of Fe^{III}-heme(NO)$^+$ (a) and of Fe^{II}-hemeH(NO)$^+$ (b). The insert in each panel shows an enlarged portion of the spectrum in the 1650–1950 cm^{-1} range. The spectra of the ^{15}NO-labeled species, drawn in grey, evidence the red shift of σ(NO).

spectrum is characterized by two distinct features at 1754 cm^{-1} and 1842 cm^{-1} in the higher frequency region. In this region the C=O stretching modes of the two propionic acid functionalities are expected. However, the mode associated to the NO stretching vibration is most interesting because its frequency is especially revealing of the electronic and structural features of the heme nitrosyl interaction. In order to assign the NO stretching vibration the IRMPD spectrum of the ^{15}NO complex has been recorded revealing no significant difference with respect to the spectrum of the unlabeled species except for the feature at 1842 cm^{-1}. This band is clearly isotope-sensitive and displays a red shift to 1810 cm^{-1}, consistent with an NO diatomic oscillator (insert in Fig. 5a). In contrast, the position of the carbonyl stretch, remains at ca. 1750 cm^{-1}. A similar experiment has been performed on the NO adduct of Fe^{III}-hemeH$^+$ ions [18] and the details of the IRMPD spectrum in the high energy region are also displayed in Fig. 5b. The unlabeled species reveals a prominent band at 1720 cm^{-1} with a distinct shoulder at 1752 cm^{-1} and only the former band is red-shifted upon ^{15}NO-labeling, moving to ca. 1694 cm^{-1}. One may infer that in naked, five coordinate heme nitrosyl complexes the NO stretching resonance is at 1720 cm^{-1} in the ferrous heme complex and at 1842 cm^{-1} in the ferric one. The NO stretching vibration is a sensitive probe of the heme–NO interaction, revealing geometrical and electronic features. As a reference, the NO molecule, a radical with an odd electron in an antibonding π* orbital, displays a stretching frequency at 1876 cm^{-1}. Removal of this electron strengthens the bond and ν(NO) moves to 2345 cm^{-1} in the case of NO$^+$. A value of ν(NO) below 1700 cm^{-1} has been found characteristic of nitrosyl iron(II) complexes [29]. The typically tilted geometry of the FeNO unit is associated to the overlap of the iron d_{z^2} orbital with the π* orbital of NO. So the nitrosyl iron(II) heme complex may be assigned the contribution of a $Fe^{III}NO^{\bullet}$ resonance structure with appreciable π* electron density on the nitrosyl ligand. In contrast, nitrosyl iron(III) complexes are characterized by a linear FeNO unit and exhibit ν(NO) above 1800 cm^{-1}. The observed NO stretching frequency at 1842 cm^{-1} provides also strong indication for coordination at the N-end of the molecule because an isonitrosyl isomer would absorb at a distinctly lower frequency.

Interaction of anions with π-acidic aromatics: direct evidence for anionic σ-complexes

In the second topic of this account, recent studies are reported illustrating the structural features of negatively charged adducts of π-acidic aromatics examined in an environment, the gas phase, that is very different from the solid state of the early crystal structures or from the solution routinely analyzed by NMR spectroscopy. As already noted in the seminal studies by Kebarle and coworkers on the gas phase equilibria for the addition of anions to substituted benzenes based on high pressure mass spectrometry [30], ascertaining the structure of anion-arene adducts has presented a challenging task [31]. In our work we have examined the binding features of a prototypical electron-deficient aromatic system [1,3,5-trinitrobenzene (TNB)] with exemplary anions (OH^-, OCH_3^-, $OC_2H_5^-$, F^-, Cl^-, Br^-, I^-, CN^-) in the gas phase using the combined information deriving from collision induced dissociation experiments at variable energy, IRMPD spectroscopy and quantum chemical calculations. The first spectroscopic evidence about the existence of a covalently bound anionic σ-complex in the gas phase has been obtained by delivering TNB-CH_3O^- ions into the gas phase by ESI of a basic methanol solution of TNB [24]. The so-formed ions have been assayed in the 900–1700 cm^{-1} range where prominent signatures associated to the symmetric stretching vibrations of the nitro groups are expected. Structural insight is gained by comparing the experimental IRMPD spectrum with the IR spectra calculated for plausible candidate structures (Fig. 6). Conceivable structures for the TNB-OCH_3^- complex that are found to lie in an energy minimum are shown in Fig. 6. The covalent anionic σ-complex is the most stable isomer (**1**). However, two non-covalent complexes may also be envisioned, whereby a methanol molecule interacts with the 1,3,5-trinitrophenyl anion, by a hydrogen bond involving either the negatively charged carbon (**2**) or a

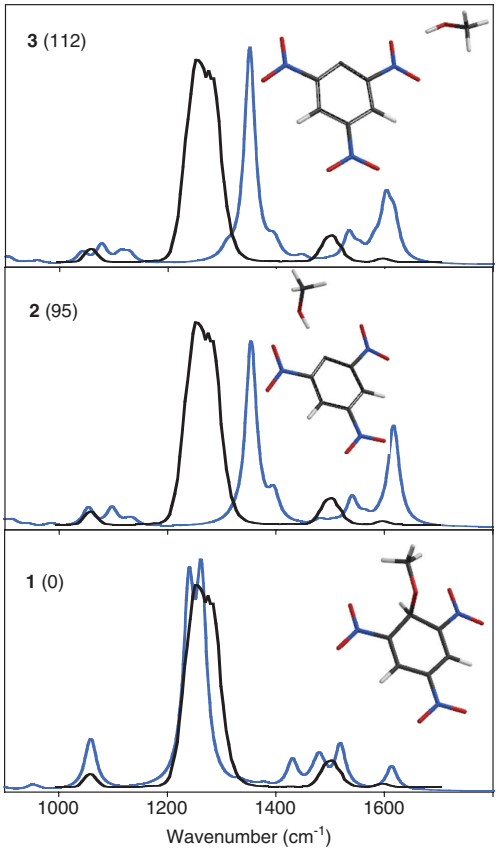

Fig. 6: IRMPD spectrum of TNB-OCH_3^- ions (black line) and calculated IR spectra (blue line) for isomers **1–3**. Quantum chemical calculations run at B3LYP/6-311++G(d,p) level of theory. Relative energies (in parentheses) are reported at 0 K in kJ mol^{-1}.

nitro group (**3**). The non-covalent complexes are markedly less stable than the σ-complex and the calculated IR spectra are very different from the experimental IRMPD spectrum (Fig. 6). The highly active symmetric stretching vibrations of the nitro groups are degenerate at ca. 1370 cm^{-1} in the calculated IR spectrum of TNB while they are redshifted and separated by ca. 25 cm^{-1} in the IR spectrum of the σ-complex. In this species the strongly covalent C–OCH_3 bond removes the degeneracy of the symmetric stretching vibrations of the nitro groups, the two ortho nitro groups being active at somewhat lower frequency, possibly related to a larger extent of negative charge delocalized onto them. The broad signature at 1253 cm^{-1} in the IRMPD spectrum is well accounted for by the unresolved features calculated at 1261 and 1285 cm^{-1} in the anionic σ-complex. The non-covalent complexes are clearly not present in any detectable amount because their spectra display bright vibrational modes in regions of the IRMPD spectrum that are void of any appreciable signal. The IRMPD spectra of the TNB-OH^- and TNB-$OC_2H_5^-$ complexes present very comparable features with the ones just described for the TNB-OCH_3^- species, with the characteristic broad and intense band ascribed to the symmetric stretching of the nitro groups appearing at 1234–1268 and 1250 cm^{-1}. Thus, IRMPD spectroscopy has provided for the first time conclusive evidence for the existence of Meisenheimer complexes in the gas phase (see Fig. 2 with X = H and Y = OH, OCH_3, OC_2H_5) [23, 24].

Strongly to weakly covalent σ-interaction in the negatively charged adducts of π-acidic aromatics

The formation of a σ-complex from the addition of an anion to an electron-deficient aromatic system represents just one, albeit prototypical, interaction motif between the two units as already evident from the alternative structures shown in Fig. 6 for the TNB-OCH_3^- complex. In recent years, a notable amount of reports have described the anion π-interaction as a new binding motif. The interaction in a π-complex is weaker than in a σ-complex and difficult to ascertain in solution [32, 33]. Conceivably, however, the anion approach to binding with a π-acidic system may span a continuity of motifs depending on the individual features of the anion and of the aromatic partner [34]. In this respect, an interesting series of structural variability is offered by the halide adducts with TNB. Candidate structures have been searched by DFT calculations and are displayed in Fig. 7 for the exemplary TNB–Br^- complex. Relative energies are also shown. Interestingly, the most stable

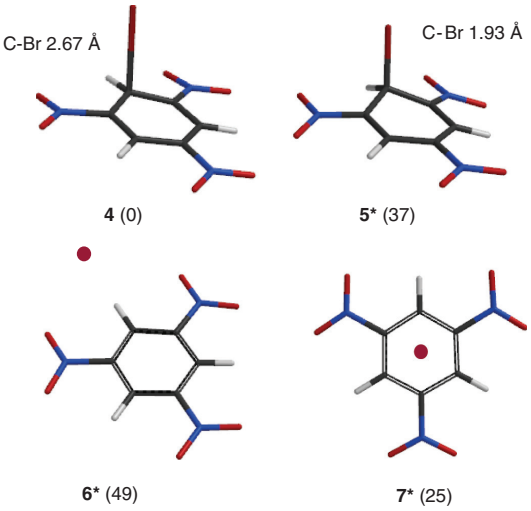

Fig. 7: Computed geometries for TNB-Br^- isomers **4–7**. Quantum chemical calculations run at B3LYP/6-311++G(d,p) level of theory. Asterisk indicates the species is not a minimum on the potential energy surface at the stated level of theory [23]. Relative energies (in parentheses) are reported at 0 K in kJ mol^{-1}.

species presents an off-center geometry, that has been described as a weak σ-motif and appears to be the preferred binding mode for the interaction of bromide ion with strongly electron deficient aromatic systems [34]. X-ray diffraction data have been reported showing that in the crystal structure a halide is placed over the periphery of the ring of strongly electron deficient arenes. Geometrical features that characterize the TNB–Br^- complex **4** are an elongated C–Br bond (2.67 Å) if compared with a typical covalent C–Br bond length (1.93 Å) and a H–C–Br angle close to 90° while the carbon atom closest to Br is not appreciably distorted from the original sp^2-type geometry [23]. Forcing this carbon to attain a tetrahedral coordination, as in a strongly covalent anionic σ-complex **5**, and constraining the C–Br distance to 1.93 Å yields a structure noticeably higher in energy relative to **4** that is not a stationary point on the potential energy surface. Also a π-centered complex (**7** in Fig. 7) with imposed C3v symmetry is not an energy minimum, characterized by two degenerate imaginary frequencies. Another alternative structure in Fig. 7 corresponds to a non covalent complex where Br^- lies in the plane of TNB and is involved in hydrogen bonding with a ring proton, **6**. Discriminating between different structures is allowed by comparing the calculated IR spectra for the potential isomers with the experimental IRMPD spectrum of the adduct as described for the TNB–OCH_3^- complex.

The calculated spectrum of **4** provides consistent matching with the IRMPD spectrum characterized by a prominent feature at 1330 cm^{-1} associated with the symmetric stretching vibrations of the nitro groups. Notably, the band is less wide and blue-shifted with respect to the corresponding spectral feature of the TNB–OCH_3^- complex. This finding is in agreement with a complex where the TNB unit is perturbed only to a limited extent by the interaction with the anion and in fact the band approaches the transition of neutral TNB at 1367 cm^{-1} [21]. If the structure of the naked TNB–anion complex is affected by the basicity of the anion, a smooth variation may be expected in the halide series from the most basic F^- (GB = 1530 kJ mol^{-1}) to the least basic I^- (GB = 1294 kJ mol^{-1}) [35]. A trend is indeed fulfilled emerging from the IRMPD spectra of the TNB–halide series reported in Fig. 8. Each experimental spectrum is plotted together with the calculated IR spectrum for the ground state structure of the complex. The geometries of the TNB–halide complexes, also depicted in Fig. 8, vary from a strongly covalent anionic σ-complex for TNB–F^- (**8**), where the F-bonded carbon has attained full sp^3 hybridization, to the weakly covalent σ-complex for TNB–I^- (**10**), with a scarcely perturbed TNB moiety. It is interesting to notice that the diagnostic position of the feature associated to symmetric stretching vibrations of the nitro groups is closest to the one for neutral TNB in the case of TNB–I^- whereas it is markedly red-shifted to 1263–1292 cm^{-1} in the case of TNB–F^-. In the latter species partial splitting into two components is also well accounted for by theory. In the strongly covalent TNB–F^- adduct the negative charge is largely delocalized on the nitro groups which lessens the double bond character of the N–O bond and is responsible for the diminished vibrational transition energy. Already in the next member of the series, namely TNB–Cl^- (**9**), the nitro groups appear less perturbed and the geometry of the complex rather conforms to a weakly covalent σ-complex. So the transition from strongly to weakly covalent σ-complex in the TNB–halide series is at the F^-/Cl^- turn. Interestingly, comprehensive computational studies on the identity S_NAr reaction $X^- + C_6H_5X \rightarrow X^- + C_6H_5X$ have shown that in the X = F, Cl, Br, I series only in the case of X = F is a $C_6H_5X_2^-$ σ-complex formed as discrete intermediate [36, 37]. The C_{2v} structures of $C_6H_5X_2^-$ (X = Cl–I) are instead transition structures. A key parameter in this trend has been recognized to be the Lewis basicity of the X^- nucleophile (markedly dropping from F^- to Cl^-) and this same factor is likely responsible for the observed change in bonding and structural features in the TNB–X^- adducts.

Carbon–carbon bond formation in ESI-formed adducts of π-acidic aromatics

The cyanide ion (CN^-, GB = 1435 kJ mol^{-1}) provides another example of strongly basic anion. However, cyanation of aromatic compounds in solution withstands the drawback of requiring highly toxic reagents. Unexpectedly, ESI mass spectrometry has offered a mild route to the formation of TNB–CN^- complexes by directly submitting to ESI in the negative ion mode an acetonitrile solution of TNB [22]. In order to solve the

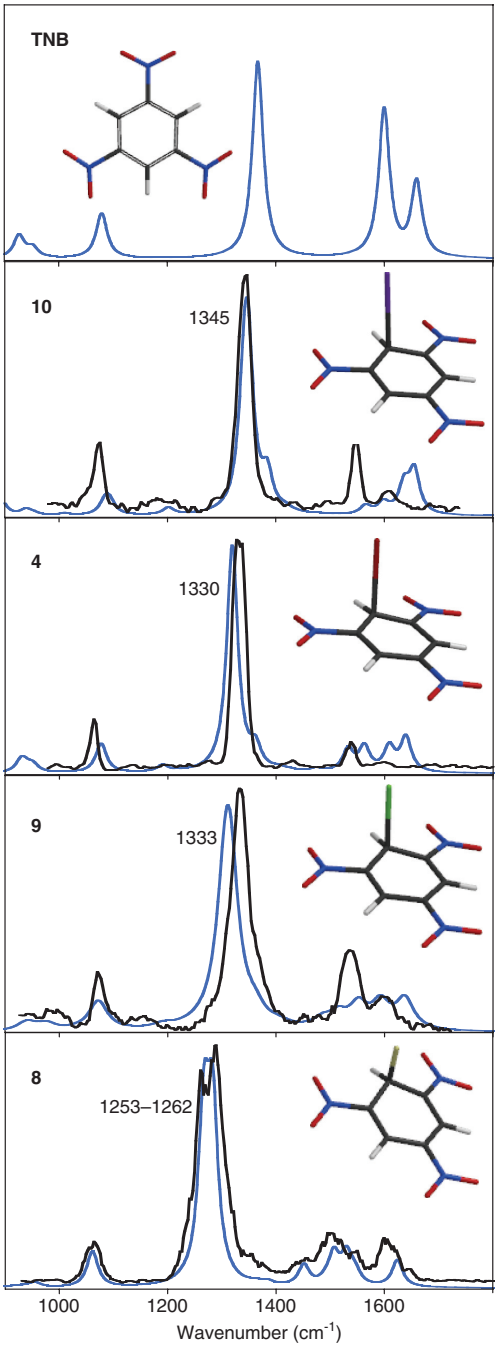

Fig. 8: IRMPD spectra (in black) of TNB-halide$^-$ ions and calculated IR spectra (in blue) for the stable isomers **4** (halide = Br^-) and **8–10** (halide = F^-, Cl^-, and I^-, respectively). For comparison purposes also the calculated IR spectrum of TNB is reported. Quantum chemical calculations run at B3LYP/6-311++G(d,p) level of theory.

structure of the so-formed species, IRMPD spectroscopy has been performed revealing the typical features of a strongly covalent σ-complex. In particular, a broad (90 cm^{-1} width at half maximum) band at 1244 cm^{-1} is accounted for by the modes at 1272 and 1245 cm^{-1} (symmetric stretching vibrations of para and ortho nitro groups, respectively) in the calculated IR spectrum of the σ-complex formed by addition of CN^- to an unsubstituted carbon of TNB. The complex is thus characterized as a Meisenheimer complex stabilized by the three nitro groups in ortho/para positions, effectively delocalizing the negative charge. Other isomeric candidates have been inspected by DFT computations. For example, cyanide attack at a nitro-substituted

carbon yields a species which on geometry optimization evolves to C–NO_2 bond cleavage and subsequent binding of nitrite to an adjacent carbon by an oxygen atom. However, no matching is provided between the experimental IRMPD spectrum and the calculated IR spectrum for this structure or other non covalently bound isomers. IRMPD spectroscopy thus confirms the ability to solve the structure of a gaseous ionic species in a straightforward way.

Conclusion

The tools of gas phase ion chemistry, including FT-ICR mass spectrometry for kinetic and thermodynamic studies of ionic reactions and IRMPD spectroscopy combined with ab initio calculations for structural insights about ionic intermediates, provide valuable information to interpret chemical properties and reactivity behavior. The two examples illustrated in the present contribution have addressed the NO adducts of iron porphyrin complexes and the addition complexes of anions with TNB, a prototypical electron deficient arene. The kinetics and thermodynamics of NO binding to iron(II)- and iron(III)-heme, where the metal is placed in a fully comparable coordination environment, namely four-coordinate by the porphyrin dianion, display a very comparable behavior. This finding sheds conclusive light on the factors affecting the remarkably higher affinity for NO by iron(II)-hemes probed in protic solvents or in a protein, which is to be traced to the presence of a vacant or labile axial coordination site. The gas phase has allowed an ideal environment where the vibrational signature of the NO ligand can be ascertained in both ferrous and ferric hemes. Inquiries about ferric hemes face the problem of undesired reductive nitrosylation when the complex is formed by NO addition in condensed phase.

IRMPD spectroscopy has yielded the first direct evidence for the existence of Meisenheimer complexes, or strongly covalent anionic σ-complexes, in the gas phase. Depending on the nature of the anion, the TNB complex may display a variable bonding geometry, as evidenced in the TNB–halide series. The ensuing structural information may hopefully provide new clues for the design of anion carriers in biological environments. It may be foreseen that IRMPD spectroscopy could aid to solve cases where anion binding is weak and NMR shifts too small to be appreciated.

Acknowledgments: This work was supported by the Università di Roma La Sapienza, by the Italian Ministry of Education, University and Research (MIUR) and by the European Community's Seventh Framework Programme for access to the CLIO FEL beamline.

References

[1] P. B. Armentrout. *Int. J. Mass Spectrom.* (2014) DOI: 10.1016/j.ijms.2014.04.005.
[2] V. M. Bierbaum. *Int. J. Mass Spectrom.* (2014) DOI: 10.1016/j.ijms.2014.07.021.
[3] P. E. Williams, B. J. Jankiewicz, L. Yang, H. I. Kenttämaa. *Chem. Rev.* **113**, 6949 (2013).
[4] Z. Tian, S. Kass. *Chem. Rev.* **113**, 6986 (2013).
[5] F. Tureček, R. R. Julian. *Chem. Rev.* **113**, 6691 (2013).
[6] H. Schwarz. *Angew. Chem. Int. Ed.* **50**, 10096 (2011).
[7] J. Roithová, D. Schröder. *Chem. Rev.* **110**, 1170 (2010).
[8] M. N. Eberlin. *Eur. J. Mass Spectrom.* **13**, 19 (2007).
[9] E. Uggerud. *Eur. J. Mass Spectrom.* **13**, 97 (2007).
[10] A. Wanat, M. Wolak, L. Orzel, M. Brindell, R. van Eldik, G. Stochel. *Coord. Chem. Rev.* **229**, 37 (2002).
[11] P. C. Ford. *Inorg. Chem.* **49**, 6226 (2010).
[12] A. Ghosh, Editor. *The Smallest Biomolecules: Diatomics and Their Interactions with Heme Proteins*, Elsevier, Amsterdam (2008).
[13] O. Chen, S. Groh, A. Liechty, D. P. Ridge. *J. Am. Chem. Soc.* **121**, 11910 (1999).
[14] B. Chiavarino, M. E. Crestoni, S. Fornarini, C. Rovira. *Chem. Eur. J.* **13**, 776 (2007).
[15] F. Angelelli, B. Chiavarino, M. E. Crestoni, S. Fornarini. *J. Am. Soc. Mass Spectrom.* **16**, 589 (2005).

[16] B. Chiavarino, M. E. Crestoni, S. Fornarini, C. Rovira. *Inorg. Chem.* **47**, 7792 (2008).
[17] B. Chiavarino, M. E. Crestoni, S. Fornarini, F. Lanucara, J. Lemaire, P. Maitre, D. Scuderi. *ChemPhysChem* **9**, 826 (2008).
[18] F. Lanucara, D. Scuderi, B. Chiavarino, S. Fornarini, P. Maitre, M. E. Crestoni. *J. Phys. Chem. Lett.* **4**, 2414, (2013).
[19] F. Lanucara, B. Chiavarino, M. E. Crestoni, D. Scuderi, R. K. Sinha, P. Maitre, S. Fornarini. *Inorg. Chem.* **50**, 4445 (2011).
[20] F. Terrier. *Modern Nucleophilic Aromatic Substitution*, Wiley, Weinheim (2013).
[21] B. Chiavarino, M. E. Crestoni, P. Maitre, S. Fornarini. *Int. J. Mass Spectrom.* **354–355**, 62 (2013).
[22] B. Chiavarino, P. Maitre, S. Fornarini, M. E. Crestoni. *J. Am. Soc. Mass Spectrom.* **24**, 1603 (2013).
[23] Barbara Chiavarino, M. E. Crestoni, S. Fornarini, F. Lanucara, J. Lemaire, P. Maitre, D. Scuderi. *Chem. Eur. J.* **15**, 8185 (2009).
[24] B. Chiavarino, M. E. Crestoni, S. Fornarini, F. Lanucara, J. Lemaire, P. Maître. *Angew. Chem. Int. Ed.* **46**, 1995 (2007).
[25] J. Olah, J. N. Harvey. *J. Phys. Chem. A* **113**, 7338 (2009).
[26] S. Shaik, H. Chen. *J. Biol. Inorg. Chem.* **16**, 841 (2011).
[27] M. E. Crestoni, S. Fornarini. *Angew. Chem. Int. Ed.* **51**, 7373 (2012).
[28] B. Chiavarino, M. E. Crestoni, S. Fornarini, F. Lanucara, J. Lemaire, P. Maitre, D. Scuderi. *Int. J. Mass Spectrom.* **270**, 111 (2008).
[29] W. R. Scheidt, M. K. Ellison. *Acc. Chem. Res.* **32**, 350 (1999).
[30] G. W. Dillow, P. Kebarle. *J. Am. Chem. Soc.* **110**, 4877 (1988).
[31] J. M. Garver, Z. Yang, S. Kato, S. W. Wren, K. M. Vogelhuber, W. C. Lineberger, V. M. Bierbaum. *J. Am. Soc. Mass Spectrom.* **22**, 1260 (2011).
[32] M.Giese, M. Albrecht, A. Valkonen, K. Rissanen. *Eur. J. Org. Chem.* 3247 (2013).
[33] H. T. Chifotides, K. R. Dunbar. *Acc. Chem. Res.* **46**, 894 (2013).
[34] B. P. Hay, V. S. Bryantsev. *Chem. Commun.* 2417 (2008).
[35] J. E. Bartmess. "Negative Ion Energetics Data", in *NIST Chemistry WebBook, NIST Standard Reference Database Number 69*, P. J. Linstrom and W. G. Mallard, (Eds.), National Institute of Standards and Technology, Gaithersburg MD, 20899, http://webbook.nist.gov, (retrieved November 26, 2014).
[36] I. Fernandez, G. Frenking, E. Uggerud. *J. Org. Chem.* **75**, 2971 (2010).
[37] M. N. Glukhovtsev, R. D. Bach, S. Laiter. *J. Org. Chem.* **62**, 4036 (1997).